Growth and characterization of nickel oxide ultra-thin films

Abdelaziz El Boujlaidi, Nabil Rochdi, Rachid Tchalala, Hanna Enriquez, Mohamed Rachid Tchalala, Andrew Mayne, Hamid Oughaddou

Growth and characterization of nickel oxide ultra-thin films

Abdelaziz El Boujlaidi[a], Nabil Rochdi[a], Rachid Tchalala[b], Hanna Enriquez[b], Andrew J. Mayne[b], and Hamid Oughaddou[b,c]

[a] *SIAM, Faculty of Sciences Semlalia, Cadi Ayyad University, Prince Moulay Abdellah avenue, PO Box 2390, 40000 Marrakesh - Morocco*

[b] *Institut des Sciences Moléculaires d'Orsay, ISMO-CNRS, Bât. 520, Université Paris-Sud, 91405 Orsay, France*

[c] *Département de Physique, Université de Cergy-Pontoise, 95031 Cergy-Pontoise Cedex, France*

*Corresponding author: Abdelaziz El Boujlaidi

E-mail address: a.elboujlaidi@uca.ac.ma

Phone number: +212 (0) 524 434 649

Fax number: +212 (0) 524 436 769

Abstract

The oxidation of the Ni(111) surface under ultrahigh-vacuum conditions is studied experimentally with low-energy electron diffraction and high-resolution X-ray photoelectron spectroscopy. Exposure of the clean Ni(111) surface to molecular oxygen at room temperature followed by annealing at 400 K leads to the formation of two different structures (2×2) and $\left(3\sqrt{3}\times 3\sqrt{3}\right)\mathrm{R}30°$, prior to the formation of the NiO(111) monolayer. The O 1s core levels indicate that the obtained oxide is terminated by oxygen atoms while the valence band measurements clearly reveal the band gap of NiO. The energy difference between the Fermi level and the maximum of the valance band is extracted and is found to be 0.47 eV.

Keywords: Nickel oxide; NiO(111) monolayer; oxygen coverage; low-energy electron diffraction; high-resolution X-ray photoelectron spectroscopy.

1. Introduction

Over the last few decades, great effort has been made to develop new methods to grow oxide films for their applications in catalysis [1, 2], solar cells [3, 4] as well as in electronic devices [5-7]. Indeed, oxides can serve either as catalytic materials or as inert supports for catalytic metal clusters [2]. In addition, oxide thin films have a strong impact on the field of nano-electronics [5-7] since they can be used as tunneling barriers for ferroelectric memories [6] and magnetic devices [7, 8]. The structure of these memories, in particular those based on polarized-electron tunnel transport, are extremely complex because they require the stacked ferromagnetic metal layers to be separated by an insulating layer of nanometric size. This insulating barrier, generally formed by a layer of 1 to 2-nm-thick dielectric oxide, must have a high homogeneity, both in composition and thickness in order to avoid leakage currents, which can drastically modify the values of the magnetoresistance [5]. In addition, anti-ferromagnetic films such as nickel oxide (NiO) films are used as spin valves to pin the magnetization of ferromagnetic films [9]. For all these reasons, it is mandatory to synthetize oxide thin films with high quality. Previously, we have studied the growth of ultrathin oxide films using atomic layer deposition and oxidation process [10-15]. In this process, one atomic monolayer (ML) of a metallic element is deposited, followed by oxidation through the exposure to molecular oxygen at room temperature (RT), and then annealed in ultrahigh vacuum (UHV) conditions. This process is repeated to obtain the required thickness of the oxide. However, even though oxide films obtained by this process present good homogeneity and good thermal stability [10, 11], they remain limited in

terms of integration in industrial technology in which high-speed material processing is required.

In this paper, we present results of the growth of a NiO ultrathin film by direct oxidation of a Ni(111) substrate. NiO layers were characterized using Low-Energy Electron Diffraction (LEED) and High-Resolution X-Ray Photoelectron Spectroscopy (HR-XPS). The structural and chemical properties of the obtained thin films were studied as function of the exposure rate to molecular oxygen and their electronic behavior was investigated.

2. Experimental method

The experiments were performed on the TEMPO beam-line of the synchrotron SOLEIL in France. The beam-line is equipped with the standard tools for surface preparation and characterization: an ion gun for surface cleaning, a low-energy electron diffractometer, and a VG SCIENTA spectrometer X-ray photoelectron spectroscopy instrument with hemispherical energy analyzer. A pure commercial (111)-oriented nickel single crystal with a diameter of 10 mm, a thickness of 2 mm, and a purity of 99.999% was fixed to the sample holder using a tungsten wire. The sample was then introduced in the ultrahigh vacuum chamber with a pressure in the low 10^{-10} mbar. Prior to the oxide growth, the Ni(111) sample was cleaned by several cycles of ionic argon sputtering at 10^{-5} mbar with a typical energy of Ar^{+} ions of 600 eV, followed by annealing at 875 K until a sharp (1×1) LEED pattern was obtained. The high-resolution photoemission spectra of the O 1s core-level, as well as the valence band measurements, were performed at room temperature. Oxidation of the Ni(111)

substrate was performed by exposing the surface to molecular oxygen (O_2) with a purity of 99.998% at RT followed by an annealing at 400 K during 10 min in UHV conditions. The annealing of the sample was performed using a tungsten filament heater located in close proximity (2 mm) behind the sample holder and the temperature was measured by a pyrometer. The oxygen exposures were varied from 20 to 100 Langmuir (L), (1 L = 1×10^{-6} Torr.s). The LEED and XPS were used to control the oxidation of Ni(111) surface after each oxidation.

The incidence angle of the photon beam was 60° with respect to normal emission. The photoelectron analyzer was oriented at an angle of 90°, the acceptance angle was 15°, both with respect to the surface normal, and the energy resolution was 0.1 eV.

3. Results and discussion

Figure 1 presents LEED patterns recorded at 90 eV of the Ni(111) surface after ion sputter cleaning (Fig. 1a) and after exposure to molecular oxygen with exposure rates of 20 L (Fig. 1b), 40 L (Fig. 1c) and 100 L (Fig. 1d) followed by annealing at 400 K during 10 min. In Fig. 1b, one can clearly notice that the 20-L-exposure to O_2 produces a (2×2) superstructure with respect to the (1×1) pattern in Fig. 1a obtained immediately after the Ni(111) substrate preparation. The diffraction spots of the substrate and the (2×2) superstructure are highlighted in Figs. 1a and 1b by black circles and light-gray squares respectively. The obtained (2×2) structure was previously reported and was assigned to the adsorption of 0.25 ML oxygen [16-19].

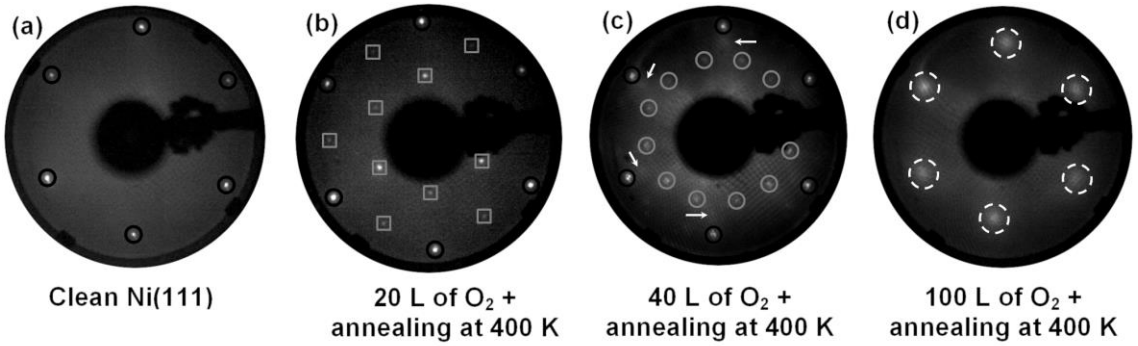

Fig. 1: LEED patterns of the Ni(111) surface recorded at 90 eV: (a) after ion sputtering cleaning, and after exposure to (b) 20 L, (c) 40 L, (d) 100 L of molecular oxygen followed by annealing at 400 K.

After exposition to 40 L of molecular oxygen followed by annealing at 400 K, the spots of the (2×2) superstructure have disappeared, and new diffraction spots are observed as shown in Fig. 1c. Some spots are identified by light-gray circles and correspond to a new structure. In addition, after exposure of Ni(111) to 40 L of oxygen, one can also distinguish additional less distinct spots (identified by the white arrows in Fig. 1c). This LEED pattern is quite similar to that observed by Munoz-Marquez et al. [21] when a clean Ni(111) surface, heated in the range of 550-600 K, receives much higher exposure rates (several cycles of 1200 L). The authors assigned the observed structure to two rotational domains of a square mesh of a NiO(100) overlayer, in rotational epitaxy with the underlying Ni(111) substrate. However, as shown in Fig. 2 corresponding to the diffraction pattern, recorded at 45 eV, of the surface after exposure to 40 L of molecular oxygen, one notices that, apart from the extra spots previously observed at 90 eV (shown in Fig. 1c), additional spots are observed. The analysis of this LEED pattern revealed that the observed spots (indicated by the dashed white lines) fit

a hexagonal mesh rotated with an angle of 30° relative to the Ni(111) crystal directions with a periodicity of $3\sqrt{3}$. Thus, the additional oxygen atoms transform the (2×2) structure obtained at 0.25 ML coverage to a $\left(3\sqrt{3}\times 3\sqrt{3}\right)\mathrm{R}30°$ superstructure (highlighted by the gray-lined grid in Fig. 2).

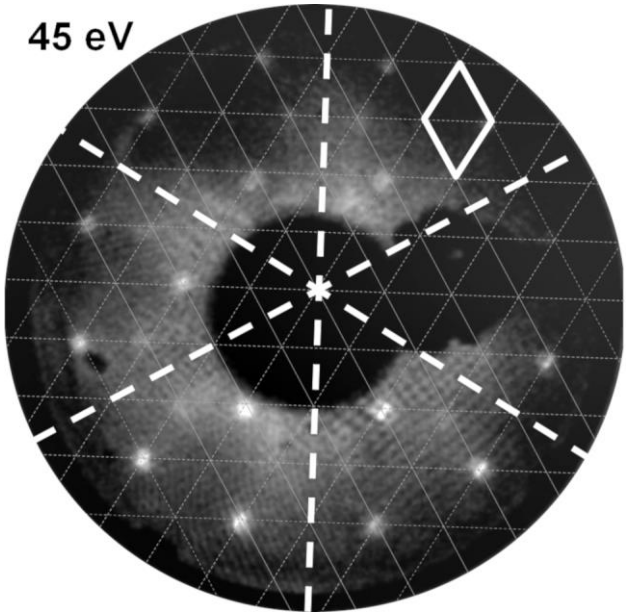

Fig. 2: LEED patterns recorded at 45 eV of the Ni(111) surface after exposure to 40 L of molecular oxygen followed by annealing at 400 K. The substrate crystal directions are indicated by dashed white lines; the $\left(3\sqrt{3}\times 3\sqrt{3}\right)\mathrm{R}30°$ superstructure is highlighted by the gray-lined grid displaying the elementary cell unit depicted in white.

The $\left(3\sqrt{3}\times 3\sqrt{3}\right)\mathrm{R}30°$ superstructure we obtained is similar to the $\left(\sqrt{3}\times\sqrt{3}\right)\mathrm{R}30°$ chemisorbed oxygen phase on Ni(111) reported previously [19]. It is consistent with a phase change in the chemisorbed oxygen structure as initially proposed by Mac Rae [20]. In addition, one can notice that there are

some missing or unclear spots in the LEED pattern of the $\left(3\sqrt{3}\times 3\sqrt{3}\right)\mathrm{R}30°$ superstructure shown in Fig. 2; which is probably due to incomplete coverage of these domains. This structure was controversial for a while as it was not always observed. It is possible that it forms as an intermediate phase at relatively small oxygen exposure before the onset of the NiO island growth phase [18].

After exposition at 100 L of molecular oxygen followed by annealing at 400 K, the $\left(3\sqrt{3}\times 3\sqrt{3}\right)\mathrm{R}30°$ has vanished, and a (1×1) LEED pattern of NiO with respect the bulk Ni(111) is clearly observed as depicted in Fig. 1d (by the dashed white circles) indicating ordered thin NiO(111) film. Indeed, from the LEED patterns of Fig. 1c and 1d, we deduced that the lattice parameter of the obtained thin oxide film is about 2.85 Å. This value is in agreement with the expected one for bulk NiO(111) (2.94 Å) [22]. Thus, one can interpret the less distinct spots of Fig. 1c (after 40-L-oxygen exposure) as that of the beginning of the formation of the (1×1) phase of the NiO thin film with respect to the bulk Ni(111). These spots become sharper after 100-L-oxygen exposure (Fig. 1d).

Using X-ray photoemission spectroscopy, we have characterized the NiO(111) films obtained after exposure to 100 L of oxygen and post-annealing at 400 K. Figure 3 displays an overview of the surface before and after the oxidation of Ni(111) substrate at a photon energy of 700 eV. The bare Ni(111) spectrum (lower curve in Fig. 3) presents the characteristic peaks of nickel. The O 1s core level is observed after the oxidation process (upper curve in Fig. 3). On the same curve, one can also notice the presence of oxygen Auger peaks (as identified on the curve). Two small additional peaks located respectively at 530

eV and 350 eV correspond to the Auger transitions of the tungsten wire used to hold the Ni substrate.

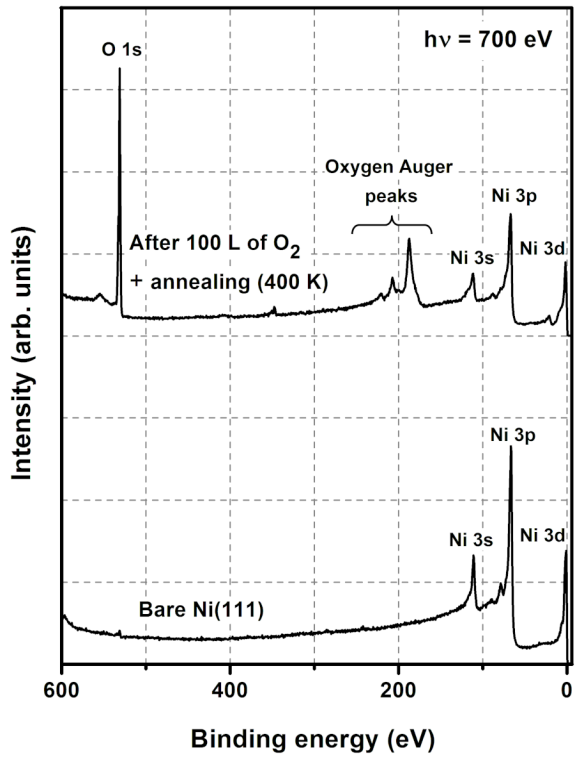

Fig. 3: XPS spectra recorded at 700 eV photon energy as a function of binding energy for the bare Ni(111) surface (lower) and after room-temperature exposure to 100 L molecular oxygen followed by annealing at 400 K (upper).

In order to estimate the thickness of the formed nickel oxide film, we calculated the mean escape depth (λ) of Ni 3p electrons detected at an angle of α = 15° with respect to the surface normal using the following equation [23]:

$$\lambda = \lambda_0 \cos\alpha \qquad (1)$$

Where λ_0 is the inelastic mean free path of electrons of Ni 3p electrons (with a kinetic energy E of 632 eV) estimated at 4.87 Å using the following equation:

$$\lambda_0 = \frac{h}{\sqrt{2m_E E}} \quad (2)$$

Where h corresponds to Planck's constant ($h \approx 6.626\times10^{-34}$ J.s), and m_E is the electron mass ($m_E \approx 9.1\times10^{-31}$ kg).

By considering the following equation [24]:

$$I = I_0 \exp\left(-d_{NiO}/\lambda\right) \quad (3)$$

Where I_0 and I refer to the XPS intensities of Ni 3p electrons measured respectively on bare Ni and after oxidation and d_{NiO} is the thickness of the NiO oxide, we can deduce a thickness value of the NiO(111) film (d_{NiO}) of about 2.91 Å ± 0.1 Å.

This value is 0.5 Å higher than the interplanar distance in bulk NiO(111) of about $4.2\ \text{Å}/\sqrt{3} = 2.42\ \text{Å}$, calculated with a lattice parameter of 4.2 Å [22]. This indicates that the thickness of the obtained NiO(111) film is between 1 and 2 layers in agreement with the model proposed by Holloway [18]. This thickness is also consistent with previous studies reporting that the formed NiO(111) is very thin and the oxidation is complete to a depth of only a few atomic layers [18, 25]. Nevertheless, one should be cautious with the estimated thickness of the nickel oxide since it was calculated under the assumption that the elastic effect can be neglected and that the emitted electrons are attenuated following inelastic scattering interactions.

Based on this XPS analysis and the estimation of the nickel oxide film thickness after 100 L of oxygen exposure, the LEED pattern of Fig. 1c (recorded after 40-

L-oxygen exposure) could be attributed to the onset formation of an ordered oxide phase of NiO(111), giving rise to the less distinct spots observed in the LEED pattern.

Figure 4 presents the valence band of the substrate recorded at a photon energy of 60 eV before and after oxidation of Ni(111) at 100 L of O_2. After the oxidation, we observe a weak intensity between 0 and 0.47 eV in comparison with that of clean Ni followed by a steady increase as the binding energy increases. The overall intensity is weaker because the photoelectrons coming from the underlying metallic Ni are strongly attenuated by the NiO layer. However, for binding energies higher than 0.47 eV, the intensity increases again. This is consistent with a contribution for the NiO valence band adding to that of the underlying Ni. This indicates the opening of a band gap of 0.47 eV of the NiO [26].

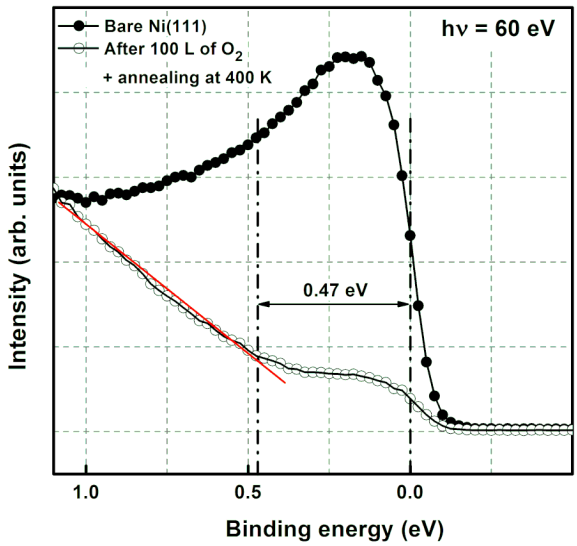

Fig. 4: Valence band of: (a) bare Ni(111) surface, (b) after exposure of Ni(111) surface to 100 L of molecular oxygen at room temperature followed by annealing at 400 K.

The exact band gap value depends on the position of the conduction band of NiO that we cannot measure since only filled states are probed in the XPS. The Fermi level is located at 0.47 eV above the top of valence band, which is consistent with the value reported in the literature (0.45 eV) [26]. Since bulk nickel oxide is a large band gap semiconductor (about 3.6-4.0 eV), the estimated energy between the Fermi level and the top of valence band indicates the obtained NiO has p-type behavior in good agreement with the literature [27-31].

The O 1s core level spectra recorded at normal and at grazing emission are shown in Fig. 5. The spectra are fitted with a Doniach-Sunjic line shape [32] with only two components S1 and S2 located respectively at 529.42 and 531.23 eV. The best fit was obtained with a 333 meV Gaussian profile and a 550 meV Lorentzian profile. The presence of two components indicates that the oxygen atoms have two chemical environments. In addition, the S2 component increases in intensity at grazing emission and decreases at normal emission indicating that the corresponding atoms are located at the surface. Thus, the S1 component is assigned to the oxygen atoms located in the NiO(111) oxide while the S2 component is assigned to oxygen atoms located at the surface. This is also in good agreement with our estimated thickness (between 1 and 2 monolayers) and with the model of NiO(111) films [33].

Let us recall that the entire process was performed under ultrahigh vacuum conditions, and the oxidation process was performed by RT exposure to pure molecular oxygen followed by post-annealing. It is generally agreed [18, 21] that

the initial ordered phases form by the dissociative chemisorption of the oxygen molecules. Nickel is commonly used as a catalyst to dissociate water, forming OH and H on the surface [35]. However, one cannot completely rule out the possibility of forming OH terminal groups at the surface of the thin film [36, 37], either via the adsorption of residual water vapor from UHV (partial pressure in the range of 10^{-11} mbar) [38] or via reaction with H radicals generated by cracking residual hydrogen in the vacuum on the ion gauge filament [39].

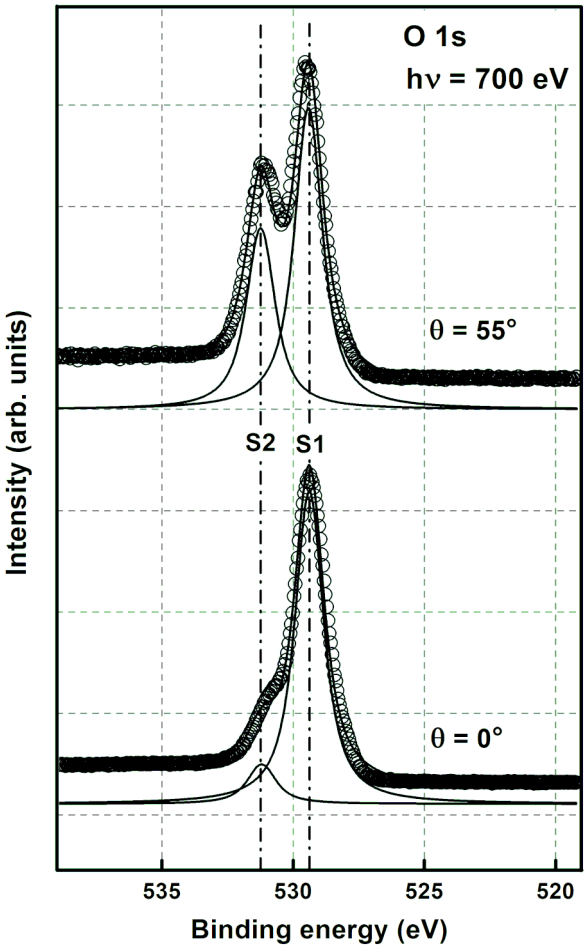

Fig. 5: O 1s core levels recorded in normal (lower) and at 55° to the surface normal after room-temperature exposure of Ni(111) to 100 L of molecular oxygen followed by annealing at 400 K (upper).

4. Conclusion

We have studied the growth of NiO(111) film by direct oxidation of a Ni(111) single crystal. Two periodic structures were observed corresponding to the partial oxidation of Ni(111). At higher coverage, a thin NiO(111) film is obtained (with an estimated thickness of one or two layers). The LEED patterns show the formation of NiO thin film with a structure similar to that of bulk NiO. The valence band measurements showed that the Fermi level is located at 0.47 eV above the top of valence band indicating a p-type behavior of the thin NiO(111) film while the O 1s core level showed that the oxide is oxygen terminated.

Acknowledgments

The authors acknowledge assistance from SOLEIL TEMPO beamline staff.

Declarations of interest:

none

Author contribution statement

The authors certify having contributed equally to the paper.

References

[1] H.-J. Freund, H. Kuhlenbeck, M. Neumann, Molecular adsorption on thin ordered oxide films and single crystal oxide surfaces, in: H.-J. Freund, E. Umbach (Eds.), Adsorption on ordered surfaces of ionic solids and thin films, Springer-Verlag, Berlin Heidelberg, 1993, pp. 136–146.

[2] C.R. Brundle, J.Q. Broughton, The initial interaction of oxygen with well-defined transition metal surfaces, in: D.A. King, D.P. Woodruff (Eds.), The chemical physics of solid surfaces and heterogeneous catalysis: Chemisorption systems, Elsevier, Amsterdam, 1990, pp. 131–388.

[3] E.A. Gibson, A.L. Smeigh, L. Le Pleux, J. Fortage, G. Boschloo, E. Blart, Y. Pellegrin, F. Odobel, A. Hagfeldt, L. Hammarström, A p-type NiO-based dye-sensitized solar cell with an open-circuit voltage of 0.35 V, Angew. Chem. Int. Ed. 48 (2009) 4402–4405.

[4] J. Zhang, H. Luo, W. Xie, X. Lin, X. Hou, J. Zhou, S. Huang,. W. Ou-Yang, Z. Sun, X. Chen, Efficient and ultraviolet durable planar perovskite solar cells via a ferrocene-carboxylic acid modified nickel oxide hole transport layer, Nanoscale 10 (2018) 5617–5625.

[5] J.S. Moodera, L.R. Kinder, Ferromagnetic–insulator–ferromagnetic tunneling: Spin dependent tunneling and large magnetoresistance in trilayer junctions, J. Appl. Phys. 79 (1996) 4724–4729.

[6] H. Takasu, Ferroelectric memories and their applications, Microelectron. Eng. 59 (2001) 237–246.

[7] S. Bhatti, R. Sbiaa, A. Hirohata, H. Ohno, S. Fukami, S.N. Piramanayagam, Spintronics based random access memory: a review, Mater. Today 20 (2017) 530–548.

[8] N. Rochdi, V. Safarov, Spin transport and precession in semiconductors in the drift-diffusion regime, J. Phys. Conf. Ser. 1081 (2018) 012002.

[9] F. Matroodi, M.G. Shoar, Giant Magnetoresistance in NiO/Co/Cu/Co/Ti spin valve fabricated by EBPVD, J. Phys. Conf. Ser. 917 (2017) 072001.

[10] H. Oughaddou, S. Vizzini, B. Aufray, B. Ealet, J.-M. Gay, J.-P. Bibérian, F. Arnaud D'Avitaya, Growth and oxidation of Al thin films deposited on Ag(111), Appl. Surf. Sci. 252 (2006) 4167–4170.

[11] S. Vizzini, H. Oughaddou, C. Léandri, V. K. Lazarov, A. Kohn, K. Nguyen, C. Coudreau, J.-P. Bibérian, B. Ealet, J.-L. Lazzari, F. Arnaud D'Avitaya, B. Aufray, Controlled growth of aluminum oxide thin films on hydrogen terminated Si(001) surface, J. Crystal Growth 305 (2007) 26–29.

[12] M. Raissi, S. Vizzini, G. Langer, N. Rochdi, H. Oughaddou, C. Coudreau, S. Nitsche, F. Arnaud D'Avitaya, B. Aufray, J.-L. Lazzari, Interfacial solid phase reactions in cobalt/aluminium-oxide/silicon(001) system, Thin Solid Films 518 (2010) 5992–5994.

[13] N. Rochdi, K. Liudvikouskaya, M. Descoins, M. Raïssi, C. Coudreau, J.-L. Lazzari, H. Oughaddou, F. Arnaud D'Avitaya, Surface morphology and structure of ultra-thin magnesium oxide grown on (100) silicon by atomic layer deposition oxidation, Thin Solid Films 519 (2011) 6302–6306.

[14] N. Rochdi, M. Raïssi, S. Vizzini, C. Coudreau, J.-L. Lazzari, B. Aufray, H. Oughaddou, F. Arnaud D'Avitaya, Structural and electrical

characterizations of nanometer scaled aluminum oxide in metal / insulator / silicon (001) heterostructures, Glob. J. Phys. Chem. 2 (2011) 230–235.

[15] H. Maradj, C. Fauquet, M. Ghamnia, B. Ealet, N. Rochdi, S. Vizzini, J.-P. Biberian, B. Aufray, H. Jamgotchian, Structure of a Zn monolayer on Ag(111) and Ag(110) substrates: An AES, LEED and STM study, Surf. Sci. 684 (2019) 44–51.

[16] L. Gragnaniello, F. Allegretti, R.R. Zhan, E. Vesselli, A. Baraldi, G. Comelli, S. Surnev, F.P. Netzer, Surface structure of nickel oxide layers on a Rh(111) surface, Surf. Sci. 611 (2013) 86–93.

[17] T.M. Christensen, C. Raoul, J.M. Blakely, Change in oxide epitaxy on Ni(111): Effects of oxidation temperature, Appl. Surf. Sci. 26 (1986) 408–417.

[18] P.H. Holloway, J.B. Hudson, Kinetics of the reaction of oxygen with clean nickel single crystal surfaces: II. Ni (111) surface, Surf. Sci. 43 (1974) 141–149.

[19] P.H. Holloway, Chemisorption and oxide formation on metals: Oxygen–nickel reaction, J. Vac. Technol. 18 (1981) 653–659.

[20] M.A. Munoz-Marquez, R.E. Tanner, D.P. Woodruff, Surface and subsurface oxide formation on Ni(100) and Ni(111), Surf. Sci. 565 (2004) 1–13.

[21] A.U. Mac Rae, Adsorption of oxygen on the (111), (100) and (110) surfaces of clean Nickel, Surf. Sci. 1 (1964) 319–348.

[22] S. Stanescu, C. Boeglin, A. Barbier, J.-P. Deville, Epitaxial growth of ultra-thin NiO films on Cu(111), Surf. Sci. 549 (2004) 172–182.

[23] S. Hoffman, Auger- and X-ray photoelectron spectroscopy in materials science, G. Ertl, H. Luth, and D.L. Mills (Eds.), Springer series in surface science 49, Springer, Heidelberg, 2013, pp. 102–104.

[24] J.E.T. Andersen, Determination of substrate and overlayer intensity ratios for metal-metal systems in AES and XPS by a crystallographic electron attenuation model, Surf. Sci. 262 (1992) 422–436.

[25] T. Okazawa, T. Nishizawa, T. Nishimura, Y. Kido, Oxidation kinetics for Ni (111) and the structure of the oxide layers, Phys. Rev. B 75 (2007) 033413.

[26] W. Zhang, H. Enriquez, Y. Tong, A. Bendounan, A. Kara, A.P. Seitsonen, A.J. Mayne, G. Dujardin, H. Oughaddou, Epitaxial Synthesis of Blue Phosphorene, Small 14 (2018) 1804066.

[27] J. Szuber, Electronic properties of the NiO (100) surface after thermal cleaning in ultrahigh vacuum, J. Electron Spectrosc. Relat. Phenom. 34 (1984) 337–341.

[28] D. Adler, J. Feinleib, Electrical and optical properties of narrow-band materials, Phys. Rev. B 2 (1970) 3112–3134.

[29] E.L. Miller, R.E. Rocheleau, Electrochemical and electrochromic behavior of reactively sputtered nickel oxide, J. Electrochem. Soc. 144 (1997) 1995–2003.

[30] G. Boschloo, A. Hagfeldt, Spectroelectrochemistry of nanostructured NiO, J. Phys. Chem. B 105 (2001) 3039–3044.

[31] Z. Wu, Y. Wang, L. Sun, Y. Mao, M. Wang, C. Lin, An ultrasound-assisted deposition of NiO nanoparticles on TiO_2 nanotube arrays for enhanced photocatalytic activity, J. Mater. Chem. A. 2 (2014) 8223–8229.

[32] J. He, H. Lindström, A. Hagfeldt, S.-E. Lindquist, Dye-sensitized nanostructured p-type nickel oxide film as a photocathode for a solar cell, J. Phys. Chem. B 103 (1999) 8940–8943.

[33] S. Doniach, M. Sunjic, Many-electron singularity in X-ray photoemission and X-ray line spectra from metals, J. Phys. C: Solid St. Phys. 3 (1970) 285–291.

[34] J.I. Flege, A. Meyer, J. Falta, E.E. Krasovskii, Self-limited oxide formation in Ni (111) oxidation, Phys. Rev. B 84 (2011) 115441.

[35] A. Mohsenzadeh, K. Bolton, T. Richards, DFT study of the adsorption of water Ni(111), Ni(110), and Ni(100) surfaces, Surf. Sci. 627 (2014) 1–10.

[36] P.R. Norton, R.L. Tapping, J.W. Goodale, A photoemission study of the interaction of Ni(100), (110) and (111) surfaces with oxygen, Surf. Sci 65 (1977) 13–36.

[37] K.S. Kim, Nicholas Winograd, X-ray photoelectron spectroscopic studies of nickel-oxygen surfaces using oxygen and argon ion-bombardment, Surf. Sci. 43 (1974) 625–643.

[38] G. Dujardin, A.J. Mayne, G. Comtet, L. Hellner, M. Jamet, E. Le Goff, P. Millet, New Model of the Initial Stages of Si(111)-(7 × 7) Oxidation, Phys. Rev. Lett. 76 (1996) 3782–3785.

[39] G. Dujardin, F. Rose, J. Tribollet, A.J. Mayne, Inelastic transport of tunnel and field emitted electrons through a single atom, Phys. Rev. B 63 (2001) 081305.